Cylindrical silicon near-IR optical amplifier driven by direct current

A. S. Abramov,[1] **I. O. Zolotovskii,**[1,2,*] **A. S. Kadochkin,**[1,2] **S. G. Moiseev,**[1,2] **D. G. Sannikov,**[1] **V. V. Svetukhin,**[3] **M. S. Yavtushenko,**[1] **and A. A. Fotiadi**[1,4]

[1]*Ulyanovsk State University, L. Tolstoy Street 42, 432017 Ulyanovsk, Russian Federation*
[2]*Institute of Nanotechnologies of Microelectronics of the Russian Academy of Sciences, Leninsky Prospekt 32A, 119991 Moscow, Russian Federation*
[3]*Scientific-Manufacturing Complex "Technological Centre," Shokin Square, House 1, Bld. 7, 124498 Zelenograd, Moscow, Russian Federation*
[4]*University of Mons, 20 Place du Parc, B-7000 Mons, Belgium*
*Corresponding author: rafzol.14@mail.ru

We propose a mechanism enabling amplification of the surface tunneling modes propagating over the semiconductor cylinder surface pumped by a direct current. Amplification of a whispering-gallery mode with a net gain as high as 10^3 cm^{-1} is demonstrated. © 2020 Optical Society of America

1. INTRODUCTION

Currently, integration of silicon electronics and photonic devices based on $A^{III}B^V$ semiconductors (gallium arsenide, indium phosphide, etc.) is among the new challenges addressed to optoelectronic engineers. However, such integration is quite costly or even impossible if only traditional tools and pure semiconductor laser techniques are exploited [1,2]. The emergence of silicon-based optical generators and amplifiers pumped by a direct current (DC) may accelerate progress in hybridization of direct and indirect gap materials. Fabrication of such sources will open up a potential route to the appearance of a new class of integrated optoelectronic devices. Integration of optical and electrical elements in such devices is attainable with the techniques underlying the production of semiconductor microchips [3].

For the last decade, the use of indirect gap semiconductors as an active laser media has been on the agenda of laser engineering. However, mainly Raman and Brillouin optical parametric generators have been considered in this context [4–9], including a Brillouin-based mode-locked laser, microwave generator, optical gyroscope, and narrowband silicon laser integrated into an optical silicon microchip [10]. Now, silicon-based laser amplifiers and generators have become emerging components of optoelectronics and integrated laser technology. In this context, design of optical amplifiers and generators driven by a direct current is of great practical importance.

In this paper, we explore the potential of n-type silicon cylinder doped with phosphorus or arsenic and pumped by a direct current demonstrating its operation as an efficient optical (near-IR) amplifier. The net gain higher than 10^3 cm^{-1} is achieved with this structure as a whispering-gallery mode (WGM) at the wavelength $\lambda = 1.55 - 1.58$ µm is used as an amplified optical signal.

2. BASIC EQUATIONS

The mechanism of optical amplification considered in this work is similar to the operational principle of the traveling wave tube (TWT) commonly used in the microwave technique [11]. To provide an effective interaction between the optical light and drift current, one has to match the phase velocity of the amplified optical wave and velocity of the current carriers. To get this matching the amplified optical wave has to be somehow slowed down. Direct current amplification of surface plasmon polaritons in nanostructures has been discussed in [12–19]. The mathematical model used here is very similar to that used previously. In particular, it has already been applied to describe SPP amplification in an ultrathin semiconductor film and in carbon nanotube pumped by a drift current reported in Refs. [12,13], respectively. Specifically, in new consideration a radius of the cylinder is much larger than the wavelength, and therefore the slowing down of the electromagnetic wave achievable in [12,13] cannot be obtained. In other words, phase matching between collinear electromagnetic and current waves is not possible anymore. Now, to satisfy the phase-matching condition the optical wave makes a spiral trajectory while propagating through the
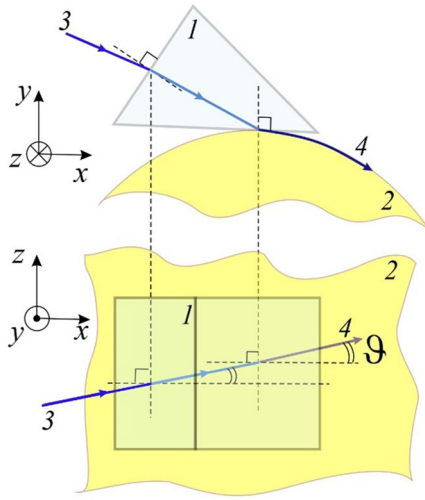
Fig. 1. Scheme of light wave introduction into the cylinder: (1) prism, (2) silicon cylinder, (3) input light, (4) optical surface wave. ϑ is the angle of light introduction onto the cylinder surface.
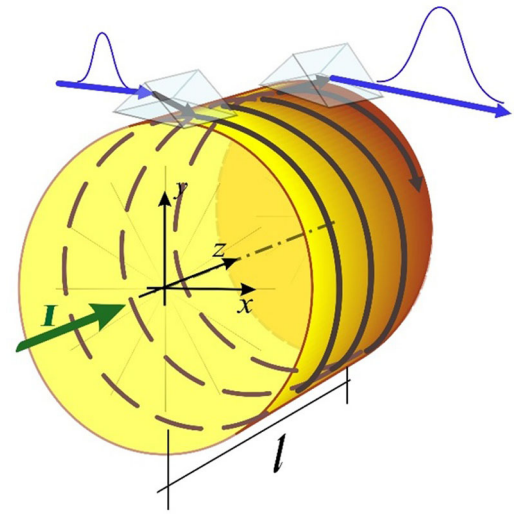

Fig. 2. Silicon cylinder with an excited optical mode (WGM). An arrow shows the current direction.

cylinder and thus enables the energy transfer from current carriers to an electromagnetic wave. To the best of our knowledge, such a process is considered here for the first time.

Let us consider an optical tunneling wave, like a WGM, propagating over the surface of a dielectric cylinder. A surface optical mode of the cylinder of a finite length is characterized by longitudinal and transverse components of the electric (magnetic) fields [20] and may interact with the ordered electric current carriers passed through the cylinder when the current carrier velocity and optical wave phase velocity are matched. In order to get such matching, the optical wave E should be introduced onto the cylindrical surface at a certain angle to the cylinder axis (Fig. 1).

In this case, it propagates over the cylinder surface on a spiral trajectory (Fig. 2). The longitudinal component of the optical propagation constant is defined as $\beta_z = (\beta_\xi^2 - \beta_\perp^2)^{1/2}$, where $\beta_\xi = n(\omega)k_0$ is the propagation constant, $\beta_\perp$ is the transverse (radial) component of the propagation constant, $k_0 = \omega/c$ is the wave number in a vacuum, and $n(\omega)$ is the refractive index (RI) of the cylinder. In this work, we assume that the cylinder is made from silicon doped with phosphorus or arsenic and $n \approx 3.4$ [21].

Interaction of an optical wave with the moving current carriers could be described by a set of two equations similar to those known from microwave theory [22–25]. The first equation describes an electromagnetic field induced by an alternative current. The harmonic component of the induced electromagnetic field at the frequency ω co-propagating with the considered optical mode (WGM) could be expressed as

$$\frac{dE}{d\xi} + i\frac{\omega}{\upsilon_{ph}}E = -\frac{1}{2}\left(\frac{\omega}{\upsilon_{ph}}\right)^2 j' K_\xi \sin\vartheta, \tag{1}$$

where υ_{ph} is the phase velocity of the electromagnetic wave; $j' \ll I_0$ is the harmonic electrical current component at ω, where I_0 is the DC current component; and ξ is the coordinate along the electromagnetic wave trajectory on the cylinder surface.

The elementary sections along the electromagnetic wave trajectory and cylinder axis z are connected as $d\xi \approx \sin\vartheta^{-1}dz \equiv Ndz$, where

$$N = 1/\sin\vartheta = \upsilon_{ph}/\upsilon_0 = c/n\upsilon_0 \tag{2}$$

is the velocity matching parameter, υ_0 is the velocity of drift current carriers, and ϑ is the angle of light input enabling corresponding to perfect matching of the optical wave phase and current carrier velocities. The coupling coefficient K_ξ in Eq. (1) describes the efficiency of the interaction between the current and optical surface wave and is defined as

$$K_\xi = \frac{\langle |E_{TM,\xi}|^2\rangle}{2\beta_\xi^2 P} = \frac{\langle |E_{TM,z}|^2\rangle}{2\beta_\xi^2 P}\sin^2\vartheta, \tag{3}$$

where $E_{TM,\xi} = E_{TM,z}/N$.

The quantities

$$P \simeq \frac{\upsilon_g n^2}{8\pi}\int_0^\infty |E|^2 dS, \tag{4}$$

$\upsilon_g = (\partial\beta_\xi/\partial\omega)_{\omega=\omega_0}^{-1}$, and $|E|^2 = |E_{TM}|^2 + |E_{TE}|^2$ are the power, group velocity, and energy (TE and TM components) of the optical wave, respectively. We can rewrite Eq. (3) introducing

$$\langle |E_{TM}|^2\rangle = \frac{1}{V_{eff}}\int_0^\infty |E_{TM}|^2 dV,$$

where $V_{eff} = (1/|E_0|^2)\int_0^\infty |E(x,y,z)|^2 dV$ is the effective optical mode (WGM) volume, dV is the elementary volume, and E_0 is the optical wave amplitude. The optical wave power given by Eq. (4) is expressed as

$$P = \frac{dW}{dt} \simeq \frac{\upsilon_g n^2}{8\pi}\int (|E_{TM}|^2 + |E_{TE}|^2)dS$$

$$\approx \frac{\upsilon_g n^2}{8\pi}\left(\langle |E_{TM}|^2\rangle + |E_{TE}|^2\rangle\right) S_{eff}^{(1)}, \tag{5}$$

where $S_{\text{eff}}^{(1)}$ is the effective optical mode (WGM) area.

Thus, with a high precision, the coupling coefficient from Eq. (3) could be approximated as

$$K_\xi \approx \frac{4\pi\eta^2}{v_g n^2 \beta_\xi^2 S_{\text{eff}}^{(1)}} \sin^2\vartheta, \qquad (6)$$

where

$$\eta = \frac{\langle|E_{\text{TM},z}|^2\rangle}{\langle|E_{\text{TM}}|^2 + |E_{\text{TE}}|^2\rangle}$$

is a fraction of the TM mode power averaged over time.

The second equation [16,22–25] in the set [i.e., solved in combination with Eq. (1)] describes the alternating current induced by the electromagnetic field. The harmonic component of the current at the frequency ω uniformly propagating along the cylinder could be expressed as

$$\frac{d^2 j'}{d\xi^2} + 2i\beta_{e\xi}\frac{dj'}{d\xi} - \left(\beta_{e\xi}^2 - \beta_p^2\right)j' = i\frac{e\beta_{e\xi}\sin\vartheta}{m_{\text{eff}}^* v_0^2} E \int j_0 dS, \qquad (7)$$

where $\beta_{e\xi} = \beta_e \sin\vartheta$, $\beta_e = \omega/v_0$ (the matching conditions), $\beta_p = \omega_p/v_0$, $\int j_0 dS = I_0$, E is the amplitude of the optical field (WGM), and e and m_{eff}^* are the charge and effective mass of the current carriers.

Now we assume that both the current fluctuation and optical mode (WGM) field vary along the waveguide length proportionally to $\exp(-ik\xi)$. In this case, solving the set of Eqs. (1) and (7) gives the following dispersion equation, similar to that reported for TWT [11,12]:

$$(\omega - kv_{ph})\left[(\omega - kv_0/\sin\vartheta)^2 - \omega_p^2\right] = C^3\omega^3, \qquad (8)$$

where

$$C^3 = K_\xi \frac{\omega_p^2 S_{\text{eff}}^{(2)}}{8\pi v_{ph}} \sin(\theta) \approx \frac{\eta^2 S_{\text{eff}}^{(2)}}{2n^2 S_{\text{eff}}^{(1)}} \frac{\omega_p^2 c^2}{\omega^2 v_g v_{ph}} \sin^3\vartheta \qquad (9)$$

and $\omega_p = \sqrt{4\pi n_0 e^2/m_{\text{eff}}^* n^2}$ is the plasma frequency. In Eq. (9) we have assumed a uniform distribution of the current density over the cylinder cross section

$$I_0 = e\int_0^\infty n_0 v_0 dS \approx en_0 v_0 S_{\text{eff}}^{(2)},$$

where $S_{\text{eff}}^{(2)} = \pi D^2/4$ is the cylinder base area and D is the cylinder diameter.

With the optical wave frequency $\omega = 2\pi c/\lambda \gg \omega_p$ lying in the near-IR spectrum range, Eq. (8) describes an increase of the optical wave field along the coordinate ξ with the gain increment

$$\alpha_\xi = \text{Im}(k) = \frac{\sqrt{3}}{2}\frac{\omega}{v_{ph}}C. \qquad (10)$$

Correspondingly, the gain increment describing optical wave amplification along coordinate z is

$$\alpha_z = \frac{\sqrt{3}}{2}\frac{\omega_0}{v_{ph}}CN \approx \frac{\sqrt{3}}{2}\left(\frac{\eta^2 n^2 \omega_p^2 \omega}{2v_g c^2}\right)^{1/3}, \qquad (11)$$

where we put $S_{\text{eff}}^{(1)} \approx S_{\text{eff}}^{(2)}$.

On other hand, the decrement describing decay of the optical wave along coordinate z is $\gamma = \beta''/\sin\vartheta$ (where β'' is the imaginary part of the propagation constant). Therefore, the net gain describing the increase of the optical wave amplitude along coordinate z is

$$G = \alpha_z - \gamma \approx \frac{\sqrt{3}}{2}\left(\frac{\eta^2 n^2 \omega_p^2 \omega}{2v_g c^2}\right)^{1/3} - \frac{v_{ph}}{v_0}\beta''. \qquad (12)$$

It is worth noting that the light absorption by free electrons is the main source of losses in the silicon at 1.55 μm [26].

With approximation $v_g \approx v_{ph} \approx c/n$, $\beta'' \approx \omega\kappa/c$, where κ is the loss decrement in silicon, the net gain given by Eq. (12) is reduced to

$$G \approx \frac{\sqrt{3}n}{2}\left(\frac{\eta^2 \omega_p^2 \omega}{2}\right)^{1/3} - \frac{\omega\kappa}{v_0 n}. \qquad (13)$$

One can see that the net gain expressed by Eq. (13) is the result of competition between the gain increment and loss decrement. Let us estimate the net gain achievable in the considered silicon structure. The typical velocity of drift current carriers in semiconductors is $v_{0\,\text{max}} \approx 10^7$ cm/s. The electron mobility in a n-type silicon with concentration of dopants (e.g., phosphorus) $n_0 \approx 10^{17}$ cm^{-3} is estimated to be $\mu_n \approx 10^3$ cm^2/(V · s) [27]. In the non-saturating regime $v_0 \approx \mu_n U/l$ and the drift current carrier velocity is connected with the applied voltage to the cylinder faces U as $U/l \approx v_0/\mu_n \approx 10^4$ V/cm. So the applied voltage as low as $U \leq 100$ V should be enough to get the effect in the cylinder with a length l shorter than 0.1 mm. With $n_0 \sim 10^{17}$ cm^{-3} and the effective electron mass $m_{\text{eff}}^* \approx 0.25 m_e$ [28], the plasma frequency is estimated to be $\omega_p \sim 10^{13}$ s^{-1}.

There are three parameters that could be adjusted to achieve the maximal net gain. They are the angle of light input onto the cylinder surface ϑ, the applied voltage U, and the cylinder length l. One can check that even with a small $\eta \sim 0.1$, very high values of the net gain could be achieved at $\lambda_0 \sim 1.55$ μm:

$$G \approx \frac{\sqrt{3}CN}{2}\frac{\omega}{v_{ph}} - \frac{\beta''c}{nv_0} \approx \frac{\sqrt{3}n}{2c}\left(\eta^2\omega_p^2\omega/2\right)^{1/3} \sim 10^3 \text{ cm}^{-1}. \qquad (14)$$

Figure 3 depicts the net gain as a function of the electron concentration in a silicon waveguide calculated from Eq. (12) for different fractions of the TM mode power $\eta = 0.1$ [Fig. 3(a)] and $\eta = 0.5$ [Fig. 3(b)]. To perform these calculations the function $\kappa(n_0)$ (see Fig. 3, inset) was estimated from the experimental data for Si waveguides [26]. Note that the presence of the dopants (As, Sb, P) of different concentration just changes the number of carriers but does not affect the function profile $\kappa(n_0)$, at least within the considered range of $10^{16} - 10^{18}$ cm^{-3}. One can see from the inset to Fig. 3 that the function $\kappa(n_0)$ is linear and all points relating to different dopants and their concentrations are lying on the same line. Within the range of the carrier concentrations $10^{17} - 10^{18}$ cm^{-3}, the net gain profile $G(n_0)$ strongly depends on the velocity matching parameter N. At small N [curves 1 and 2 in Figs. 3(a) and 3(b)], the function $G(n_0)$ exhibits a peak at the point where the loss decrement increasing with n_0 starts to compensate gain. At high N (i.e., at
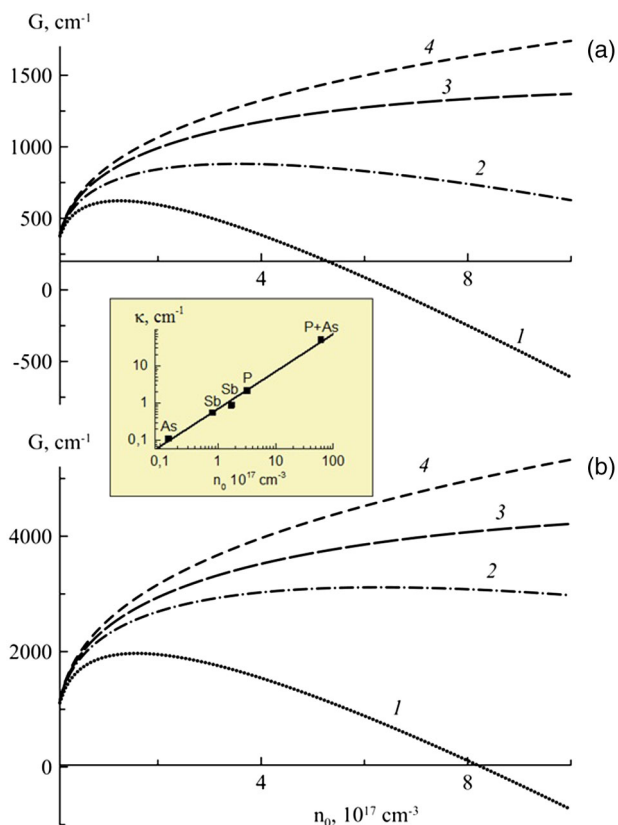
Fig. 3. The net gain $G(n_0)$ as a function of electron concentration in the doped silicon cylinder calculated for different velocity matching N. (a) Fraction of the TM mode power $\eta = 0.1$, $N = 1000$, 500, 200, 50 (curves 1–4); (b) fraction of the TM mode power $\eta = 0.5$, $N = 2500$, 1000, 500, 50 (curves 1–4). Other parameters are n = 3.4757 ($\lambda = 1$, 55 µm, T = 293 K, [21]), $m_{\text{eff}}^* = 0.25 m_e$. Yellow inset: the loss decrement $\kappa(n_0)$ as a function of the carrier concentration n_0 taken from the experimental data [26] for silicon with some different dopants and their different concentrations.

small light input angle), the net gain falls down to zero and even becomes negative [curve 1, Fig. 3(a) and 3(b)]. With a decrease of N at high drift velocities, the slope of $G(n_0)$ also decreases (curves 3 and 4). Comparison of Figs. 3(a) and 3(b) highlights the polarization sensitivity of the system. An increase of the TM mode power fraction η up to 0.5 causes a drastic increase of the net gain [Fig. 3(b)] up to several thousand cm^{-1}. Such huge values of the net gain are quite attractive and make a new design of the electrically driven silicon generators very promising.

It is worth noting that for $\beta'' < 1$ cm^{-1} with the velocity matching parameter $N = 1/\sin\vartheta \approx 10^3$, the loss decrement (along z) can be estimated as $\gamma \approx \beta'' N < 10^3$ cm$^{-1} < G$. So the optical losses are lower than the net gain G even at a small η. In this case, the amplifier is able to operate in a wide spectrum range (>1 µm in the near IR). The operating wavelength is tunable within this range through adjustment of the light input angle (e.g., using a prism).

Therefore, in order to achieve the most effective amplification in the silicon cylinder by a drift current, the concentration of dopants in silicon waveguides should be optimized. On the one hand, higher carrier concentration corresponds to a higher plasma frequency, which, in its turn, leads to a higher

net gain G [see Eq. (12)]. On the other hand, an increase of the carrier concentration decreases the charge mobility and significantly increases the optical losses resulting in the loss decrement exceeding the gain increment. For example, with the dopant concentration of $n_0 \approx 10^{18}$ cm^{-3}, the losses in the waveguide are pretty high, but the maximum drift velocity is much lower than $\upsilon_0 < 10^7$ cm/s. On the other hand, for the considered silicon structure with the concentration lower than $n_0 < 10^{16}$ cm^{-3}, a low plasma frequency provides a low gain increment.

3. CONCLUSION

In summary, we have proposed a mechanism enabling amplification of the surface tunneling modes as they propagate over the surface of a silicon cylinder pumped by a direct electric current. For the waves operating in the near-IR range, the acquired optical gain increment could exceed the optical loss decrement, resulting in a net gain G of $\sim 10^3$ cm^{-1}.

It is worth noting that instead of pumping by the direct current combined with the input angle adjustment through a prism, one can use electrical pumping by the alternating current $I = I_0[1 + \Delta_1 \cos(\Omega t - qz)]$. In this case the dielectric constant (and hence refractive index) is modulated [29,30] as $\varepsilon = \varepsilon_0[1 + \Delta_2 \cos(\Omega t - qz)]$, and so matching between the optical wave and drift carrier velocities could be achieved through adjustment of the current frequency Ω as $\Omega/q \sim \upsilon_0$. This method allows us to avoid mechanical adjustment of the light input angle by the prism. In this context, generation of the space charge waves (SCW) in a semiconductor cylinder can also be employed. SCWs or spatiotemporal perturbations of the charge density could arise in semiconductors with negative differential mobility under conditions of strong electrical fields [29,30]. The SCW propagation velocity is close to the carrier drift velocity, so this effect is suitable for self-matching of the surface optical wave and drift current.

Finally, generation of highly localized surface waves, such as surface plasmon polaritons on the surface of the cylinder, seems to be also promising for achieving ultrahigh net gain $G(z) \gg 10^3$ cm^{-1}, since the condition $\upsilon_g \to 0$ is supported by the nature of plasmon polaritons [15,16]. However, it is well beyond the scope of this paper.

Disclosures. The authors declare that there are no conflicts of interest related to this article.

REFERENCES

1. J. Leuthold, C. Koos, and W. Freude, "Nonlinear silicon photonics," Nat. Photonics **4**, 535–544 (2010).
2. Z. Fang and C. Z. Zhao, "Recent progress in silicon photonics: a review," ISRN Opt. **2012**, 428690 (2012).
3. A. A. Zadernovskiĭ and L. A. Rivlin, "Photon-phonon laser action in indirect-gap semiconductors," Quantum Electron. **23**, 300–308 (1993).

4. D. Liang and J. E. Bowers, "Recent progress in lasers on silicon," Nat. Photonics **4**, 511–517 (2010).

5. H. Rong, R. Jones, A. Liu, O. Cohen, D. Hak, A. Fang, and M. Paniccia, "A continuous-wave Raman silicon laser," Nature **433**, 725–728 (2005).

6. S. S. Iyer and Y. H. Xie, "Light emission from silicon," Science **260**, 40–46 (1993).

7. M. J. Chen, C. S. Tsai, and M. K. Wu, "Optical gain and co-stimulated emissions of photons and phonons in indirect bandgap semiconductors," Jpn. J. Appl. Phys. **45**, 6576–6588 (2006).

8. L. Pavesi, "Routes toward silicon-based lasers," Mater. Today **8**, 18–25 (2005).

9. L. Pavesi, "Silicon-based light sources for silicon integrated circuits," Adv. Opt. Technol. (2008).

10. N. T. Otterstrom, R. O. Behunin, E. A. Kittlaus, Z. Wang, and P. T. Rakich, "A silicon Brillouin laser," Science **360**, 1113–1116 (2018).

11. S. E. Tsimring, *Electron Beams and Microwave Vacuum Electronics* (Wiley, 2006).

12. Y. S. Dadoenkova, S. G. Moiseev, A. S. Abramov, A. S. Kadochkin, A. A. Fotiadi, and I. O. Zolotovskii, "Surface plasmon polariton amplification in semiconductor-graphene-dielectric structure," Ann. Phys. **529**, 1700037 (2017).

13. A. S. Kadochkin, S. G. Moiseev, Y. S. Dadoenkova, V. V. Svetukhin, and I. O. Zolotovskii, "Surface plasmon polariton amplification in a single-walled carbon nanotube," Opt. Express **25**, 27165–27171 (2017).

14. T. A. Morgado and M. G. Silveirinha, "Negative Landau damping in bilayer graphene," Phys. Rev. Lett. **119**, 133901 (2017).

15. A. S. Abramov, I. O. Zolotovskii, S. G. E. Moiseev, and D. I. Sementsov, "Amplification and generation of surface plasmon polaritons in a semiconductor film–dielectric structure," Quantum Electron. **48**, 22–28 (2018).

16. S. G. Moiseev, Y. S. Dadoenkova, A. S. Kadochkin, A. A. Fotiadi, V. V. Svetukhin, and I. O. Zolotovskii, "Generation of slow surface plasmon polaritons in a complex waveguide structure with electric current pump," Ann. Phys. **530**, 1800197 (2018).

17. D. Svintsov and V. Ryzhii, "Comment on 'Negative Landau damping in bilayer graphene'," Phys. Rev. Lett. **123**, 219401 (2019).

18. D. Svintsov, "Emission of plasmons by drifting Dirac electrons: a hallmark of hydrodynamic transport," Phys. Rev. B. **100**, 195428 (2019).

19. T. A. Morgado and M. G. Silveirinha, "Morgado and Silveirinha reply," Phys. Rev. Lett. **123**, 219402 (2019).

20. M. L. Gorodetsky, *Optical Microresonators with Giant Q-factor* [in Russian] (Fizmatlit, 2011).

21. H. H. Li, "Refractive index of silicon and germanium and its wavelength and temperature derivatives," J. Phys. Chem. Ref. Data **9**, 561–658 (1980).

22. D. I. Trubetskov and A. E. Khramov, *Lectures on Microwave Electronics for Physicists* [in Russian] (Fizmatlit, 2005).

23. L. L. Clampitt, "High-power microwave tubes," Proc. IEEE **61**, 279–280 (1973).

24. J. R. Pierce, *Electrons and Waves* (Anchor Books, 1964).

25. V. N. Shevchik, G. N. Shvedov, and A. V. Soboleva, *Wave and Oscillatory Phenomena in Electron Beams at Microwave Frequencies* (Pergamon, 1966).

26. I. I. Ukhanov, *Optical Properties of Semiconductors* [in Russian] (Nauka, 1977).

27. C. Jacoboni, C. Canali, G. Ottaviani, and A. Alberigi Quaranta, "A review of some charge transport properties of silicon," Solid State Electron. **20**, 77–89 (1977).

28. H. M. Van Driel, "Optical effective mass of high density carriers in silicon," Appl. Phys. Lett. **44**, 617–619 (1984).

29. A. A. Barybin, *Waves in Thin-film Semiconductor Structures with Hot Electrons* [in Russian] (Nauka, 1986).

30. M. Shur, *Physics of Semiconductor Devices* (Prentice Hall, 1990).